

Short Communication

Study on Mechanical and Anticorrosion Performance of NiW Alloy Coatings Prepared by Induced Codeposition

Yuhan Hu, Yundan Yu*, Hongliang Ge, Guoying Wei, Li Jiang,

College of Materials Science and Engineering, China Jiliang University, Hang Zhou 310018, China

*E-mail: yuyundan@163.com

Received: 17 October 2018 / *Accepted:* 18 November 2018 / *Published:* 5 January 2019

NiW alloy coatings were obtained from the acid solution with different concentrations of tungstate. Influences of tungsten contents on mechanical and anticorrosion performance of NiW alloy coatings were investigated. Tungsten cannot be directly deposited from aqueous solution. However, with the interaction of nickel ions, tungsten and nickel could be codeposited together considered as induced codeposition. The microstructure of NiW alloys coating is Ni₁₇W₃ with face center cubic which is a kind of solid solution with nickel as solvent and tungsten as solute. Tungsten atoms occupy the lattice points of the nickel atoms and squeeze the nickel atoms to form lattice distortion resulting in the increase of hardness. NiW alloy coatings with higher tungsten content possess denser and compact nodular structures that contribute directly to the increase of anticorrosion performance.

Keywords: NiW alloy coatings; Electrodeposition; Anticorrosion;

1. INTRODUCTION

According to a recent survey, the annual metal corrosion loss in developed countries accounts for 3-4% of GDP. Metal corrosion can cause great economic loss as well as heavy accidents. Hard chromium coatings are the most commonly used protective materials in harsh environments, which possess the advantages of high hardness, optimal anticorrosion performance and great wear resistance. Many works have been done about hard chromium coatings so far.[1-8] Although the coatings with chromium possess excellent properties, the hexavalent chromium ions are highly toxic that can badly affect people's physical fitness. At the same time, the discharge of solutions with chromium ions will lead to soil and water pollution.[9-10] The hexavalent chromium is considered as a kind of high risk toxic substances and forbidden to use in many countries. Therefore, it is of great significant to develop environmentally friendly chromium replacement coatings.

Materials of iron group elements combined with nonmetal or metallic oxide have become one of

the popular substitute chromium coatings due to their excellent mechanical and anticorrosion performance. For example, Yu investigated the corrosion resistance of CoP coatings prepared by electroless deposition.[11] NiMo alloys with excellent corrosion resistance were reported by Yang published in journal of corrosion science.[12] Deng prepared a kind of FeMo coatings with optimal wear resistance.[13] Except for the coatings reported above, it is found out that the iron group elements combined with tungsten also possess excellent properties. Tungsten is a silver white metal with high hardness and melting point which does not react with any strong acids at ambient temperature. Therefore, the unique nature of tungsten makes it available in the applications of space, aircraft, metallurgy and so on. In the paper, NiW alloy coatings with various amounts of tungsten were prepared by plating technology to study their different microstructures, hardness, corrosion resistance and surface morphology. In addition, tungsten cannot be deposited from aqueous solution. It is known that iron group metals can be deposited together with tungsten, known as induced codeposition which is also discussed in the paper.

2. EXPERIMENTAL PART

The electrodeposition system of NiW alloy coatings was based on three electrodes. 99% pure platinum plate with $2 \times 2 \text{ cm}^2$ was used as the counter electrode while $1 \times 1 \text{ cm}^2$ size of pure copper was chosen as the working electrode. Saturated Calomel electrode (SCE) was designed as the reference electrode in the electrodeposition system of NiW alloy coatings. The surface of working electrode was polished each time before electrodeposition. Detail information about plating bath formula and technology parameters was listed in Table 1.

Table 1. Solution formula and plating parameters of NiW alloy coatings

| Solution formula and technology parameter | Value |
|---|------------------------------------|
| $\text{NiSO}_4 \cdot 6\text{H}_2\text{O}$ | 0.5 molL^{-1} |
| $\text{NaWO}_4 \cdot 2\text{H}_2\text{O}$ | $0.1\text{-}0.3 \text{ molL}^{-1}$ |
| $\text{Na}_3\text{C}_6\text{H}_5\text{O}_7 \cdot 2\text{H}_2\text{O}$ | 2 molL^{-1} |
| T | 353 K |
| pH | 8 |
| J (current density) | 2 Adm^{-2} |
| pH | 4 |
| t (plating time) | 1800 s |

NiW alloy coatings were obtained based on the plating parameters listed in table 1 from the bath of 200 ml. Electrochemistry station (Parstat 2273) was used to prepare and study electrochemistry mechanism of NiW electrodeposition. Cyclic voltammetry curves were used to investigate the electrochemistry process of Ni, W and NiW electrodeposition with 20 mVs^{-1} scanning rate. Polarization

curves were used to study the anticorrosion performance of NiW alloy films based on Tafel extrapolation in the solution of 3.5 wt.% NaCl. The polarization experiment was based on three electrodes system. Meanwhile, the NiW film ($1 \times 1 \text{ cm}^2$) and platinum sheet ($2 \times 2 \text{ cm}^2$) were chosen as working and counter electrode respectively. Saturated calomel electrode was used as the reference electrode. The scanning rate was 1 mV/s. The composition of NiW alloy coatings was analyzed by energy dispersive spectrometer (EDX1800B). Hardness of samples was measured by vickers (HVS-1000P) with 0.3 kg pressure. Scanning electron microscope (Hitachi S-4800) was chosen to observe the different surface morphology of NiW alloy coatings.

3. RESULTS AND DISCUSSION

3.1 NiW electrodeposition

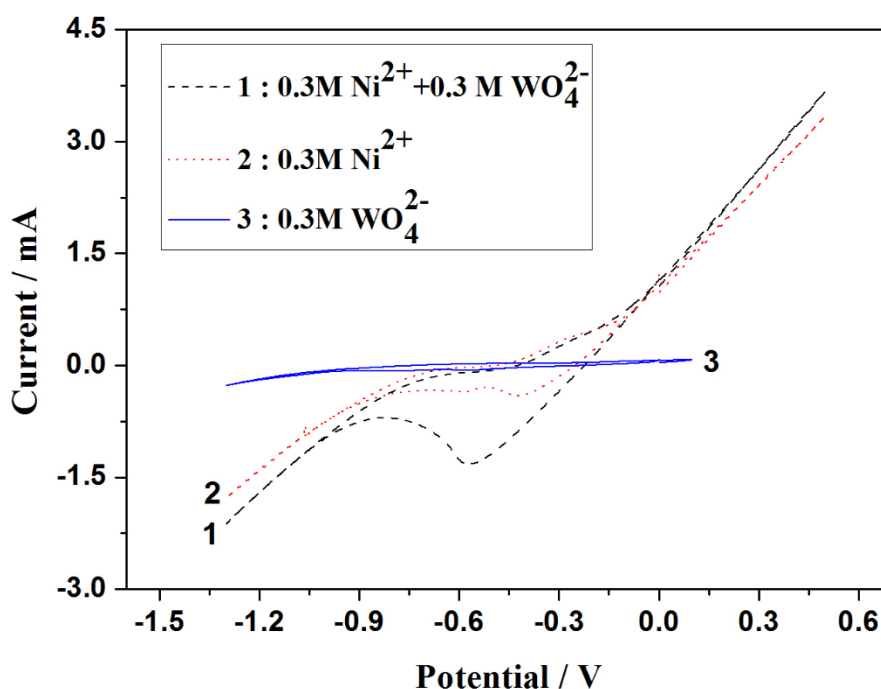


Figure 1. cyclic voltammogram of NiW, Ni and W (working electrode: 1 cm^2 pure copper sheet; counter electrode: 4 cm^2 platinum sheet; reference electrode SCE; scanning rate 20 mv/s)

According to the cyclic voltammogram of nickel, with the sweeping voltage moves to negative position, typical reduction peak of nickel is observed. Nickel ions get electrons and start to change to nickel at the potential around -0.4 V . The deposition potential of tungsten is very negative, which cannot be electrodeposited from aqueous solution directly.[14-15] Regarding to the cyclic voltammogram of tungsten, it is conspicuous that there is no typical reaction current observed with the increase of deposition potential. However, with the interaction of nickel ions, tungsten and nickel could be codeposited together considered as induced codeposition. At present, researchers have not reached a consensus on the mechanism of induced codeposition. Younes believes that a kind of metal complex, $[(\text{Ni})(\text{HWO}_4)(\text{Cit})]^{2-}$ will be formed in the electrolyte, that could be deposited in the form of sosoloid to

obtain NiW alloys.[16] Podlaha and Landolt state that[17-18], during the codeposition process of NiW alloys, a kind of adsorption product $[\text{NiCit}(\text{WO}_2)]^-$ will be obtained which is favorable to get NiW alloys. All of the above theories suggest that nickel plays a synergistic role in the deposition of tungsten, which is enhanced with the increase of citric acid and nickel ions concentration.

3.2 Composition of NiW alloy coatings

NiW alloy coatings could be codeposited from the solution with citrate. It is found out that amounts of tungsten play a big role in the properties of NiW alloy coatings. Therefore, in this sector, different NiW alloy coatings were prepared from the solutions with various concentrations of sodium tungstate. Specific information of NiW composition is shown in figure 2.

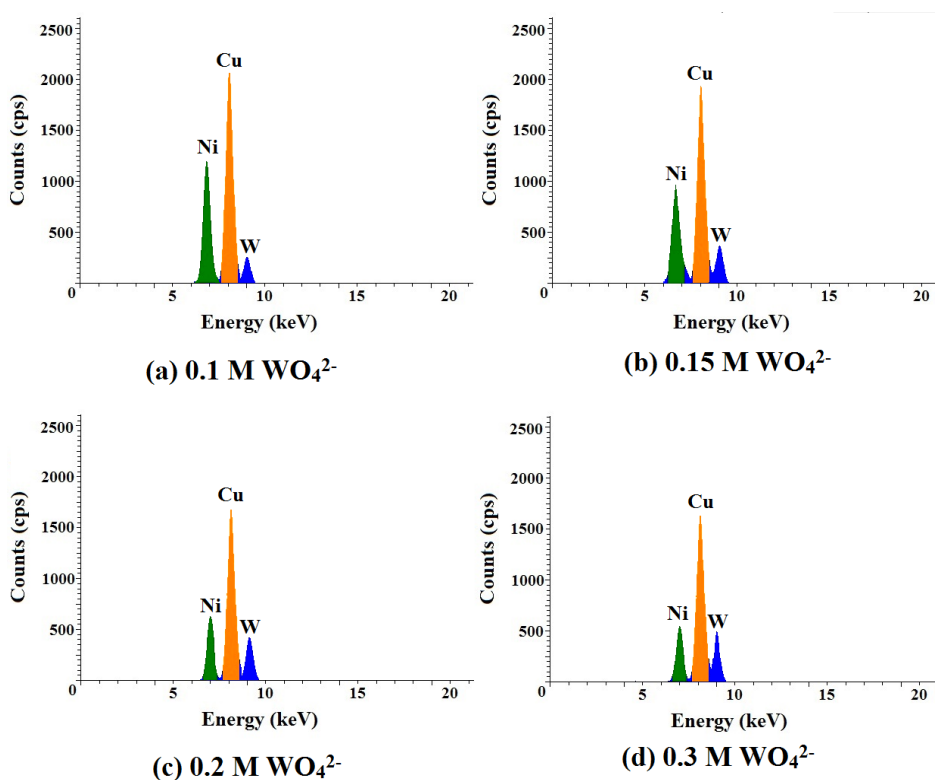
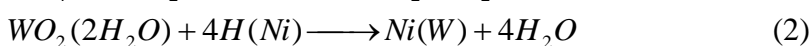
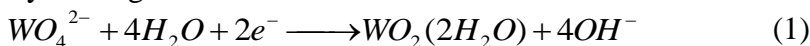


Figure 2. EDS patterns of NiW alloy coatings obtained from different concentrations of tungstate (a. 0.1 M tungstate; b. 0.15 M tungstate; c. 0.2 M tungstate; d. 0.3 M tungstate)

Three typical energy peaks representing nickel, copper and tungsten respectively are observed on the EDS pattern. With the increase of tungstate, amounts of tungsten increase gradually from 22% to 45% while the nickel contents in NiW alloys decrease. The tungsten contents of the samples obtained with different concentrations of tungstate were 22%, 32%, 39% and 45% respectively.

Therefore, it believes that the tungsten in the solution is favor to increase the tungsten content in NiW alloy coatings.



Regarding to the chemical reaction formula (1) and (2), tungstate ions are reduced to tungsten oxide, which is beneficial to form NiW alloys with interaction of nickel and nascent hydrogen. The electrochemical reaction process of NiW was investigated and discussed by many reporter.[19-21]

3.3 Microstructure and hardness of NiW alloy coatings

XRD was used to study the microstructure of NiW alloy coatings. The specific information was shown in figure 3.

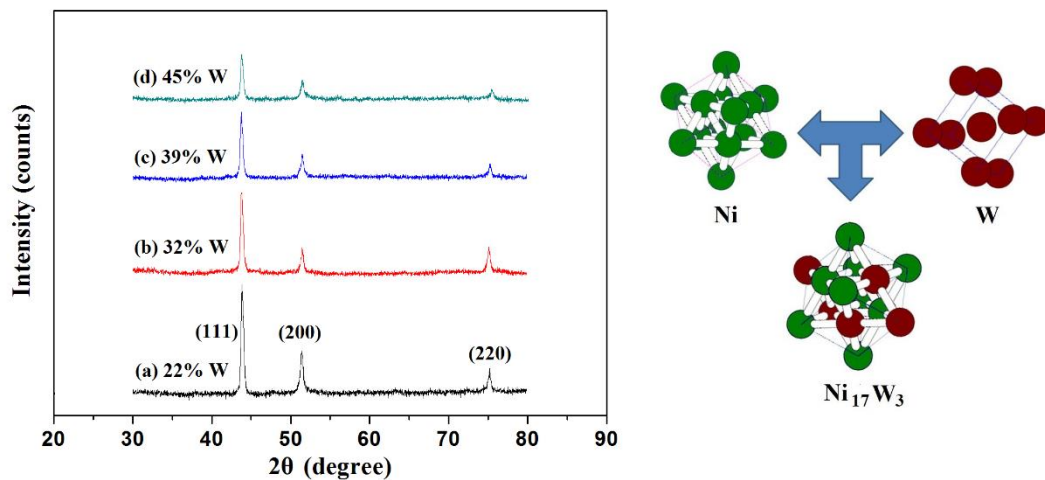


Figure 3. XRD patterns of NiW alloy coatings with different contents of tungsten. (a. NiW obtained from solution with 0.1 M tungstate; b. NiW obtained from solution with 0.15 M tungstate; NiW obtained from solution with 0.2 M tungstate; NiW obtained from solution with 0.3 M tungstate)

Three typical diffraction peaks of (110), (200) and (220) are detected on the XRD patterns at $2\theta=44.03^\circ$, $2\theta=51.26^\circ$ and $2\theta=75.23^\circ$ respectively which illustrated the Ni_{17}W_3 structure. With the increase of tungsten contents in the NiW alloy coatings, the intensity of diffraction peaks decrease gradually. Tungsten atoms occupy the lattice points of the nickel atoms and squeeze the nickel atoms to form lattice distortion. The lattice distortion phenomenon decreases grain size of the NiW alloy coating resulting in the decline of diffraction peaks. The crystal cell structures of Ni, W and NiW alloys are also shown in figure 3. The same structure of NiW alloys was also reported in some works.[22-23]

The Vickers hardness device was used to test the hardness of NiW alloy coatings with different amounts of tungsten. The testing pressure was maintained at 0.3 kg for each specimen. The value of hardness was calculated based on the testing pressure and size of indentation.

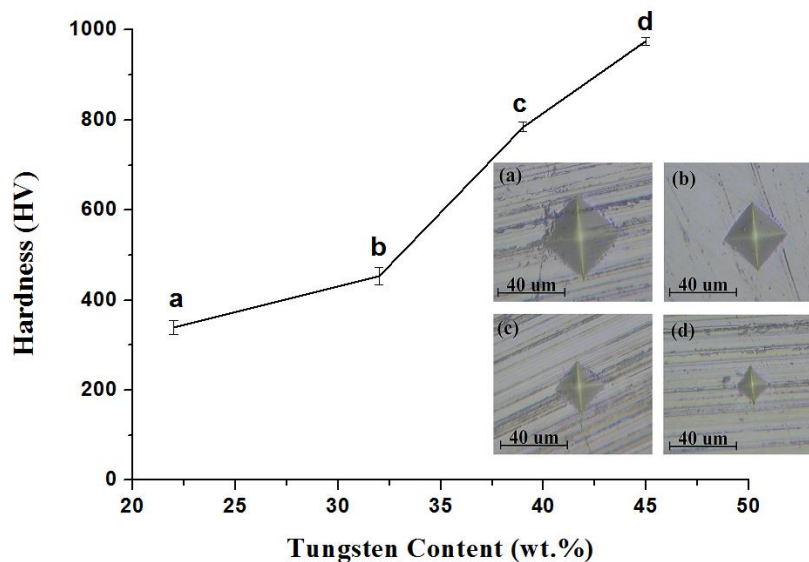


Figure 4. Hardness of NiW alloy coatings (a. sample with 22% W; b. sample with 32% W; c. sample with 39% W; d. sample with 45% W;)

As can be seen from figure 4, the hardness of NiW alloys increases greatly with the rise of tungsten contents. When the tungsten content is about 45%, the hardness of the coating can reach to about 950 HV. Because of the high hardness of metallic tungsten, the addition of tungsten significantly increases the hardness of NiW coatings. The NiW alloy coating is a kind of solid solution structures with nickel as solvent and tungsten as solute. The lattice node of nickel atom is occupied by tungsten atom. The higher the content of tungsten in the coating, the greater the lattice distortion will be caused which contributes to the increase of hardness.

3.3 Anticorrosion performance and surface morphology of NiW alloy coatings

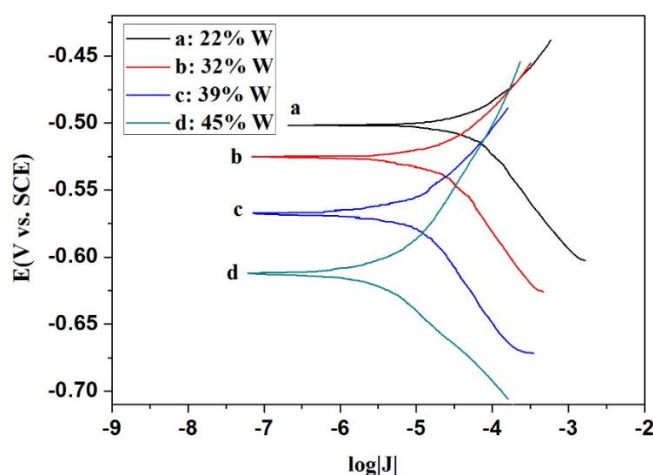


Figure 5. Polarization curves of NiW alloy coatings (scan rate 3 mv/s; scan potential from -0.7 to -0.45 V; corrosion solution 3.5 wt.% NaCl)

Electrochemistry station was used to analyze the anticorrosion performance of NiW alloy coatings based on polarization curves in the bath with 3% mass percent sodium chloride.

According to the figure 5, it is clear that NiW alloy coatings with various tungsten contents possess different Tafel curves. Detail information about corrosion potential and current density is listed in Table 2.

Table 2. corrosion parameters of NiW alloy coatings

| Tungsten content (wt.%) | Corrosion potential (V) | Corrosion current density ($\mu\text{A}/\text{cm}^2$) | Tafel slope b_a (mv/dec) |
|-------------------------|-------------------------|---|----------------------------|
| 22% | -0.502 | 32.5 | 60.1 |
| 32% | -0.526 | 18.7 | 80.9 |
| 39% | -0.568 | 11.2 | 107.2 |
| 45% | -0.612 | 8.3 | 163.3 |

With the increase of tungsten contents, the NiW alloy coatings possess more negative self corrosion potential and less corrosion current density. The incorporation of tungsten atoms decreases the grain size of NiW alloy coatings to form denser surface that contribute directly to the decline of corrosion current density. Moreover, the Tafel slope b_a ranged from 60.1 to 163.3 mv/dec since the tungsten contents increased gradually.

In order to investigate the effect of tungsten contents on the surface morphology of NiW alloy coatings, SEM images of samples are shown in figure 6.

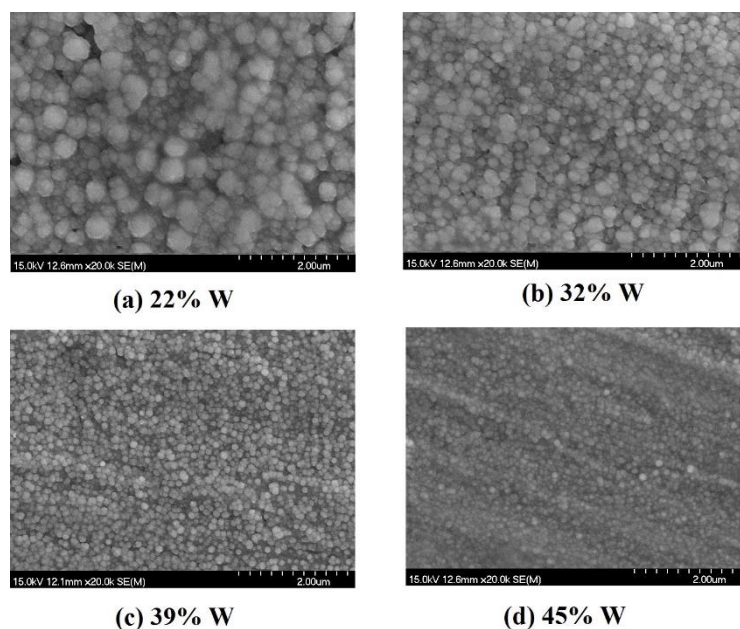


Figure 6. Surface morphology of NiW alloy coatings with 20 k magnification

The NiW alloy is a kind of typical granular coatings composed of nodular structures. Coatings with higher tungsten contents possess smaller and denser particles with uniform surface. The lattice distortion phenomenon caused by the incorporation of tungsten atoms decreases the grain size of NiW

alloy coatings resulting in the denser and compact surface morphology.

4. CONCLUSION

NiW alloy coatings with different tungsten contents were electrodeposited in the paper. The effect of tungsten on microstructure, hardness, anticorrosion and surface morphology of NiW alloy coatings was investigated. It was found out that, NiW alloy coatings could be codeposited from the solution with citrate. The amounts of tungsten play a big role in the properties of NiW alloy coatings. Improving the concentration of tungsten in the solution is favor to increase the tungsten content in NiW alloy coatings. NiW alloy coating is a kind of solid solution structures with nickel as solvent and tungsten as solute, considered as Ni_{17}W_3 . The lattice node of nickel atom is occupied by tungsten atom. The higher the content of tungsten in the coating, the greater the lattice distortion will be caused which contributes to the increase of hardness. NiW alloy coatings with higher tungsten content possess denser and compact nodular structures resulting better anticorrosion performance.

ACKNOWLEDGEMENT

This paper is supported by Science and technology plan projects of Zhejiang province (2018C37043), and Open project of key laboratory (2018K05).

Reference

1. F.F. Wang, L.J. Zheng, Q.S. Li and F.X. Zhang, *Surf. Coat. Technol.*, 349 (2018) 392.
2. N. Wint, A.C.A.D. Vooys and H.N. McMurray, *Electrochimica. Acta.*, 203 (2016) 326.
3. F.F. Wang, F.X. Zhang, L.J. Zheng and H. Zhang, *Appl. Surf. Sci.*, 423 (2017) 695.
4. Y. Yin, C.L. Pan, R.H. Zhang and C. Zhao, *J. Alloys Compd.*, 765 (2018) 782.
5. D.Q. Zhao, X. Jiang, Y.X. Wang and W.S. Duan, *Appl. Surf. Sci.*, 457 (2018) 914.
6. L. Lu, Z. Zhang, Y.C. Guan and H.Y. Zheng, *Opt. Laser Technol.*, 106 (2018) 272.
7. H. Zaw and P. Muangjunburee, *Mater. Today Proc.*, 5 (2018) 9281.
8. A.H. Yaghtin, E. Salahinejad, A. Khosravifard and A. Araghi, *Ceram. Int.*, 41 (2015) 7916.
9. M. Shahid, S. Shamshad, M. Rafiq and S. Khalid, *Chemosphere*, 178 (2017) 513.
10. B. Kiran, N. Rani and A. Kaushhik, *J. Environ. Chem. Eng.*, 4 (2016) 4137.
11. Y.D. Yu, Z.L. Song, H.L. Ge and G.Y. Wei, *Prog. Nat. Sci.*, 24 (2014) 232.
12. C. Yang, O. Muransky. H.L. Zhu and I. Karatchevtseva, *Corros. Sci.*, 143 (2018) 240.
13. X.K. Deng, G.J. Zhang, T. Wang and S. Ren, *Surf. Coat. Technol.*, 350 (2018) 480.
14. E.B. Lehman, A. Bigos, P. Indyka and A. Chojnacka, *J. Electroanal. Chem.*, 813 (2018) 39.
15. M. F. Zhang, C.F. Zhu, C.P. Yang and Y. N. Lv, *Surf. Coat. Technol.*, 346 (2018) 40.
16. O. Younes and E. Gileadi, *J. Electrochem. Soc.*, 149 (2002) 1.
17. E.J. Podlaha and D. Landolt, *J. Electrochem. Soc.*, 143 (1996) 885.
18. E.J. Podlaha and D. Landolt, *J. Electrochem. Soc.*, 143 (1996) 893.
19. E. Slavcheva, W. Mokwa and U. Schnakenberg, *Electrochimica. Acta*, 28 (2005) 5573.
20. P. Salehikahrizangi, K. Raeissi and F. Karimzadeh, *Surf. Coat. Technol.*, 344 (2018) 626.
21. M.Y. Wang, Z. Wang and Z.C. Guo, *Mater. Lett.*, 64 (2010) 1166.
22. M.Y. Wang, Z. Wang and Z.C. Guo, *Mater. Chem. phys.*, 148 (2014) 245.

23. M.P. Quiroga, S.B. Ribotta, M.E. Folquer and E. Zelaya, *Electrochimica. Acta*, 72 (2012) 87.

© 2019 The Authors. Published by ESG (www.electrochemsci.org). This article is an open access article distributed under the terms and conditions of the Creative Commons Attribution license (<http://creativecommons.org/licenses/by/4.0/>).